

# Energetic Drivers to Augment Cellular Physiology: Towards a New Paradigm

Jacqueline A. Bonds<sup>1,2\*</sup>, Ramamurthy Chitteti<sup>1,2\*</sup>, Elena L. Kopp<sup>1,2\*</sup>, and Juan P. Zuniga-Hertz<sup>1,2\*</sup>

<sup>1</sup>*Department of Anesthesiology, University of California, San Diego, La Jolla, United States*

<sup>2</sup>*Veterans Affairs San Diego Healthcare System, La Jolla, United States*

\*Authors contributed equally

## Abstract

Living organisms, from the simplest organization to the more complex ones, all share the requirement of energy in order to perform basic functions that allow homeostatic functions to maintain life and ensure endurance and resilience. Cellular physiology requires complex mechanisms to maintain homeostasis that are activated when normal parameters change. Ancient medical practices like acupuncture suggest that many human health impairments occur because of an energetic imbalance. In this regard, over the last 35 years, NES Health has coined the concept of Energetic Drivers as sub-fields of energy that power the body. Since the cell is the most basic living unit, those fields must also apply and can be externally modulated when out of balance by the imprinting of determined energy frequency or with various media that carry and transfer such energy. Infoceuticals are waters containing this specific information that can be imprinted with specific devices. In this report, we used a multicellular platform to determine the effect on cellular physiology of diverse infoceuticals and frequency imprinting. We observed unique and cell-specific effects in terms of cellular membrane structure, mitochondrial function, cellular proliferation, oxidative stress, and protection from viral infection. These findings aim to provide basic science insights into the process of understanding the underlying phenomena that take place with energetic drivers.

**Key words:** Infoceuticals, cell physiology, metabolism.

## Introduction

Life, from its simplest forms to higher organisms, presents common factors or functions like growth, reproduction, response to stimuli, metabolism, beside others. Also, all these functions present another common element: all require energy in order to function. Since energy cannot be created on a thermodynamic system, it is conserved through them (first law of thermodynamics) and is transformed from one form to another. Energy flows in living systems in manners which allow for its conversion and transformation for use in many processes. Such is the case for electrochemical gradients and the consequent electromotive force that leads to

synthesis of biomolecules, storage of energy in chemical structures and bonds, movement, cellular communication, and virtually all biological processes.

The same way potential energy is “stored” in a dam, the generation of gradients throughout the cellular membranes is used to accumulate potential energy, giving cellular membranes a cornerstone role in life. For this reason, membranes can be referred to as energetic capacitors [1]. During the geological eras, membranes evolved into complex systems which based on their biochemical composition, with greater emphasis in their lipids and proteins, have permitted complex forms of life and all the underlying bioenergetic mechanisms to exist [2].

However, it is critical to understand that energy can assume diverse forms, ranging from potential energy, chemical energy, electricity, and many others.

Holistic medicine practices and techniques, such as acupuncture, suggest the existence of energetic fields [3, 4]. NES Health suggests the existence of Energetic Drivers (EDs) as sub-fields of energy that arise during fetal development that “powers” the body [5]. In this regard, the EDs can be modulated using Infoceuticals, water formulations which have been subjected to specific electromagnetic frequencies and thus contain various types of energetic information that can differentially affect living cells *in vitro* [6]. NES Health has accumulated knowledge over the years regarding infoceuticals, and it is based on empirical evidence supporting the ability to match the function of EDs imprinted with the information carried by an infoceutical and the corresponding acupuncture point in the body.

In order to obtain quantifiable results on how various infoceuticals are impacting cellular physiology, we performed a battery of *in vitro* experiments using various types of cells: cardiac muscle, skeletal muscle, neural stem cells, and lung epithelial cells. This study investigates potential effects on biophysical parameters such as membrane rigidity and fluidity, mitochondrial ultrastructure and metabolism, cellular proliferation, and the potential to provide protection to viral infections. The aim of the study is to determine the extent to which various infoceuticals modulate general aspects of the cell physiology and behavior *in vitro*.

## Methods

### *Cell culture*

C2C12 (CRL-1772<sup>TM</sup>), H9C2 (CRL-1446<sup>TM</sup>), and A-549 (CRM-CCL-185) cell lines were purchased from American Type Culture Collection (ATCC, Manassas, VA, USA). C2C12 cells (mouse myoblast) and H9C2 cells (cardiomyoblasts from embryonic rat hearts)

were cultured in Dulbecco’s Modified Eagle’s Medium (DMEM) (GIBCO/BRL, 11885092) containing 5mM glucose, supplemented with 10% Fetal Bovine Serum (FBS, Thermo Fisher Scientific, 16000044) and 1% Penstrep (Penicillin/Streptomycin, GIBCO, 15140122). All used culture media were sterile filtered with EMD Millipore Stericup Sterile Vacuum Filter Units (Fisher Scientific, SCGPU05RE). The cells were maintained in vented 75cm<sup>2</sup> tissue culture flasks (Sarstedt, Germany) and incubated at 37°C under an atmosphere of 95% air and 5% CO<sub>2</sub>. The cultures were routinely split, using trypsin (0.25% Trypsin-EDTA, Gibco, 25200-056) at 50-60% confluence. To keep the cultures in low passages, stocks were frozen in liquid nitrogen at passage one to three (DMEM with 5% DMSO). To preserve the characteristics of the cell lines, treatments of C2C12 and H9C2 myoblasts were started in passage 2-8 in all experiments.

### *Primary Neurospheres*

*Culture.* Primary neurospheres (neural stem cells) were thawed from multiple isolations (neurospheres were isolated from adult mice as previously described [7]). In brief, each vial of neural stem cells was rapidly thawed in a 37°C water bath. Cells were washed in 9mL of warm growth media (DMEM/F-12 [ThermoFisher Scientific 11320082], 1% penicillin-streptomycin, 20% B27 supplement [Gibco, 17504044], 10% N2 supplement [Gibco, 17502001]) and centrifuged at 1000rpm for 5 minutes at RT. Cells were resuspended in growth media EGF, bFGF, and noggin. Neurospheres were cultured for 7 days with growth factors (EGF, bFGF, and noggin) added every 48-72 hours.

*Passaging.* Media containing neurospheres was collected and spun at 1000 rpm for 5 minutes at RT. Neurospheres were dissociated by resuspending in 1.25 mL of 0.05% trypsin-EDTA and incubated in a 37°C water bath for 7 minutes. 3 mL of Trypsin inhibitor was added, and cells spun at 1000 rpm for 5 minutes. Cells were then

counted (BioRad Automated Cell Counter) and plated at 5,000 cells/cm<sup>2</sup> for experiments.

### **Infoceuticals treatment**

H9C2, C2C12, and A-549 were treated for 72h; cell culture media was replaced daily to add the infoceutical at specific dilutions. For neurospheres, the infoceutical was added directly to the media every 24 hours. For membrane studies, H9C2 cells were treated with ED3 Cell Driver (CD) (dilutions 1:100, 1:1,000, 1:10,000); for cellular metabolism, H9C2 and C2C12 cells were treated with ED3 Cell Driver, ES13 COH infoceutical (COH), and ED9 muscle driver (MD). To test infoceutical effects on neural stem cells, neurospheres were treated with Energy Water and COH infoceuticals. In addition, we used the NES Health imprinting device in order to treat H9C2 and A549 cells to determine the effect of ED3 and ED13 imprinting frequencies in cellular oxidative stress and viral infection protection, respectively.

### **Electron paramagnetic resonance spectroscopy membrane fluidity analysis**

After CD treatment, H9C2 cells membrane fluidity was determined by electron paramagnetic resonance spectroscopy (EPR) as previously described [2]. Briefly, cells were resuspended after 5min incubation with trypsin 0.25% at 37°C and subsequently washed in ice-cold PBS 1X. Cells were resuspended in 200mL of complete culture media, split into two 100mL aliquots and incubated with spin probes 5 and 16-Doxy stearic acid (5-DSA, 16-DSA), respectively. Cells were incubated 5min on ice and 5min at 25 °C. Un-bound spin probe was removed by subsequent wash and resuspension in fresh complete media. Samples were placed in 50mL MagneTech capillaries and analyzed in a MagneTech MiniScope MS400 benchtop spectrometer. EPR conditions include microwave power of 7mW, modulation amplitude of 2G; modulation frequency of 100kHz, sweep width of 141.21G centered at 3357.90G, and a scan rate of

7.31G/s. The spectrum of 5-DSA analysis is used to determine membrane fluidity/rigidity parameters; rotation correlation time ( $\tau$ ) of the spin probe was obtained from the 16-DSA spectrum analysis as previously described [8].

### **H9C2 Mitochondrial transmitted electron microscopy**

6-well plates of confluent cells were fixed with 1% glutaraldehyde, 4% paraformaldehyde in 0.1M cacodylate buffer for 1 hour at room temperature and overnight at 4°C. After washing, the cells were post-fixed with 1% OsO<sub>4</sub> and *en bloc* stained with 2% uranyl acetate for one hour each. After dehydration through a standard ethanol series, cells were transitioned with hydroxypropyl methacrylate (HPMA; Ladd Scientific #21328) to LX-112 (#21310 Ladd Scientific) and embedded as monolayers. After polymerization at 60°C, pieces of monolayers were mounted on blocks using superglue and dried overnight prior to sectioning. Sections of 70-75nm were stained with uranyl acetate and lead nitrate before viewing on Tecnai T-12. Mitochondria from all cell areas, plasma membrane-associated, perinuclear and free cytosolic populations were randomly sampled. Mitochondrial count and area calculations were analyzed with ImageJ software.

### **BrdU Cell Proliferation Assay**

Neurospheres were single-cell dissociated using trypsin as described above. Cells were counted and plated at 5000 cells/well in a 96-well plate. This assay was performed using a commercially available kit from BioVision (BrdU Cell Proliferation Assay Kit, K306). In brief, 5-Bromo-2'-dioxyuridine (BrdU) was diluted to 1X in each well and cells cultured for 24 hours. Plates were centrifuged at 1000 rpm for 5 minutes and the manufacturers protocol was followed.

### **Viral infection analysis**

To test the effect of infoceuticals preventing viral infection, A549 cells were plated in 96-well plates ( $5 \times 10^5$  cells/well) and treated with imprinter set at ED13 (Immunity Enhancer Infoceutical) for 90 seconds over the course of 72 hours days. Subsequently, cells were treated with an engineered viral construct consisting in HIV virus where the genetic material was replaced by red fluorescent protein (RFP) expression system and the SARS-CoV2 virus Spike protein (Beta, Delta, UK, D614G, Lambda, and Brazil variants) infection system. When the viral construct (Pseudo-Covid virus) infects a lung cell, the RFP is expressed in the cytosol, and red fluorescence can be measured as a means of viral infection. Red fluorescence was measured after 24h of viral exposure in a Tecan Spark 10M fluorescence plate reader at 535-590nm. Red fluorescence was normalized by nuclear staining with DAPI. Values are expressed as RFP/DAPI. In addition, live immunofluorescence imaging of A549 cells was performed. The red fluorescence is an indicator of cells that were infected. DAPI was used as nuclear staining control.

### **Reactive oxygen species analysis**

To evaluate the effect of the ED3 imprinting frequency (cellular energy, metabolism, and communication) in cellular oxidative stress due to reactive oxygen species (ROS), we cultured H9C2 cells on a glass-bottom 96-well plate (Cellvis-P96) and treated the cells ( $3.5 \times 10^6$  cells) with the imprinter set at ED3 frequency for 90 seconds over the course of 72 hours. After the last day, cells were incubated with CellROX $\alpha$  green ROS detection reagent at final concentration of  $1\mu\text{M}$  per well for 4 to 6 hrs at  $37^\circ\text{C}$ . After completion of incubation, the cells were washed with PBS 1X. The ROS mean signal intensity was quantified using Citation 5 (Bioteck) and images in software (Gen5).

### **Mitochondrial membrane potential**

Mitochondrial general health was measured by determining the mitochondrial membrane potential (MMP). H9C2 cells were treated with ED3 imprinting (90 seconds over 72 hours) and the infoceutical water preparation. The MMP measurement was performed with the Mito-ID Membrane Potential Cytotoxicity kit (Enzo Life Sciences, Farmingdale, NY). The ROS mean signal intensity was quantified using Citation 5 (Bioteck) and images in software (Gen5). The green fluorescence reports MMP loss and an impaired mitochondrial health; the orange fluorescence reports healthy mitochondria.

### **Analysis**

All results are expressed as mean  $\pm$  SD and analyzed by one-way ANOVA variance test followed by Tukey's test for multiple comparison. A  $p$  value  $<0.05$  was considered as a statistically significant difference.

## **Results**

### ***Chronic cell driver infoceutical treatment induces cellular membrane biophysical changes***

The cellular membranes are more complex than the mere boundaries of the cell. They behave like organelles with complex and dynamic structural organization that controls the internal environment of the cell, substances exchange, communication, besides others. In order to evaluate possible effects of the cell driver infoceutical in cellular membranes, we treated H9C2 cells with three different dilutions of the cell driver infoceutical and studied membrane biophysical parameters like fluidity and rigidity in different regions of the lipid bilayer (i.e., near the polar headgroups and the hydrophobic core) by electron paramagnetic resonance spectroscopy (EPR). To assess membrane fluidity and rigidity near the polar head groups of the lipid bilayers, we used 5-doxyl stearic acid (**Fig. 1A**). We observed an increase in the rigid/fluid ratio in the cells treated with  $10^4$  dilution of cell driver infoceutical ( $1.06 \pm 0.035$ ,  $n=5$ ) (**Fig. 1C**).

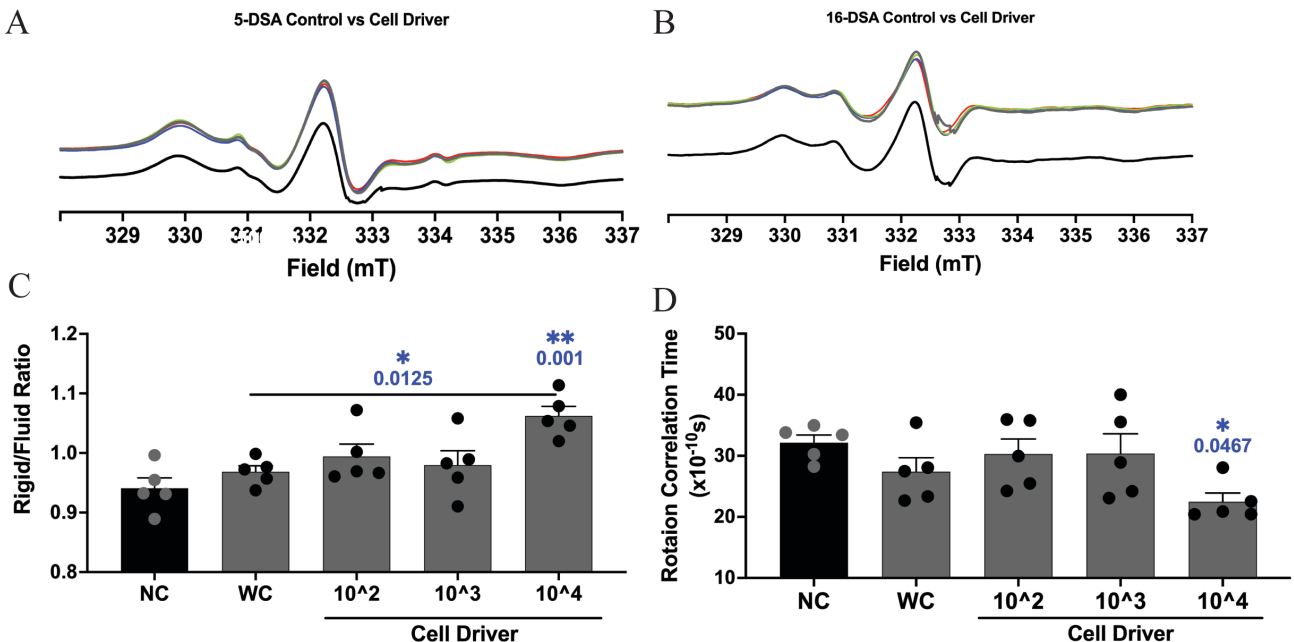


**Figure 1: CD infoceutical modifies H9C2 cellular membrane parameters.** EPR spectra of 5-DSA (A) and 16-DSA (B). Black line, negative control (NC); gray line, water control (WC); green line, CD  $10^2$  dilution; blue line, CD  $10^3$  dilution; red line, CD  $10^4$  dilution. (C) Rigid/Fluidity ratio of cell membranes two-components spectra analysis (n=5). (D) Rotational correlation time (Tcorr) of 16-DSA was calculated to evaluate the membrane rigidity in the hydrophobic region of the lipid bilayer

Interestingly, by using 16-doxyl stearic acid (Fig. 1B), we observed a reduction in rotational correlation time, suggesting an increase the fluidity of the hydrophobic core of the lipid bilayers ( $22.47 \pm 3.24$ , n=5) (Fig. 1D). These results suggest that chronic exposure to cell driver infoceutical induced changes in the cellular membranes that can be associated with distinct cellular functions.

#### **Chronic cell driver infoceutical treatment promotes mitochondrial health in H9C2 cells**

To investigate mitochondrial structural effects of CD infoceutical, we studied mitochondrial morphology through transmitted electron microscopy. After 72h treatment with CD at three different dilutions, mitochondrial inspection (Fig. 2A) in H9C2 cells showed a significant difference in mitochondrial numbers *per cell* (Fig. 2B), without changes in mitochondrial area (Fig. 2C). These data suggest that CD may

induce mitochondrial fusion and fission dynamics, increasing their number.

MMP can be used as a measure of the general state of the mitochondria. The loss of mitochondrial membrane potential is associated with early stages of apoptosis. We measured the MMP by using two stains where the green fluorescence signal is an indicator of the loss of MMP and the orange signal refers to a healthy mitochondrion. We observed that after the treatment of the cells with ED3 infoceutical, there were no increases in green signal but a reduction in orange (compared to the water control), suggesting a mild reduction in mitochondria health (Fig. 2D, E).

#### **COH infoceutical induces mouse neural stem cells proliferation**

Stem cell proliferation has been one of the key cellular events that have been studied due to its

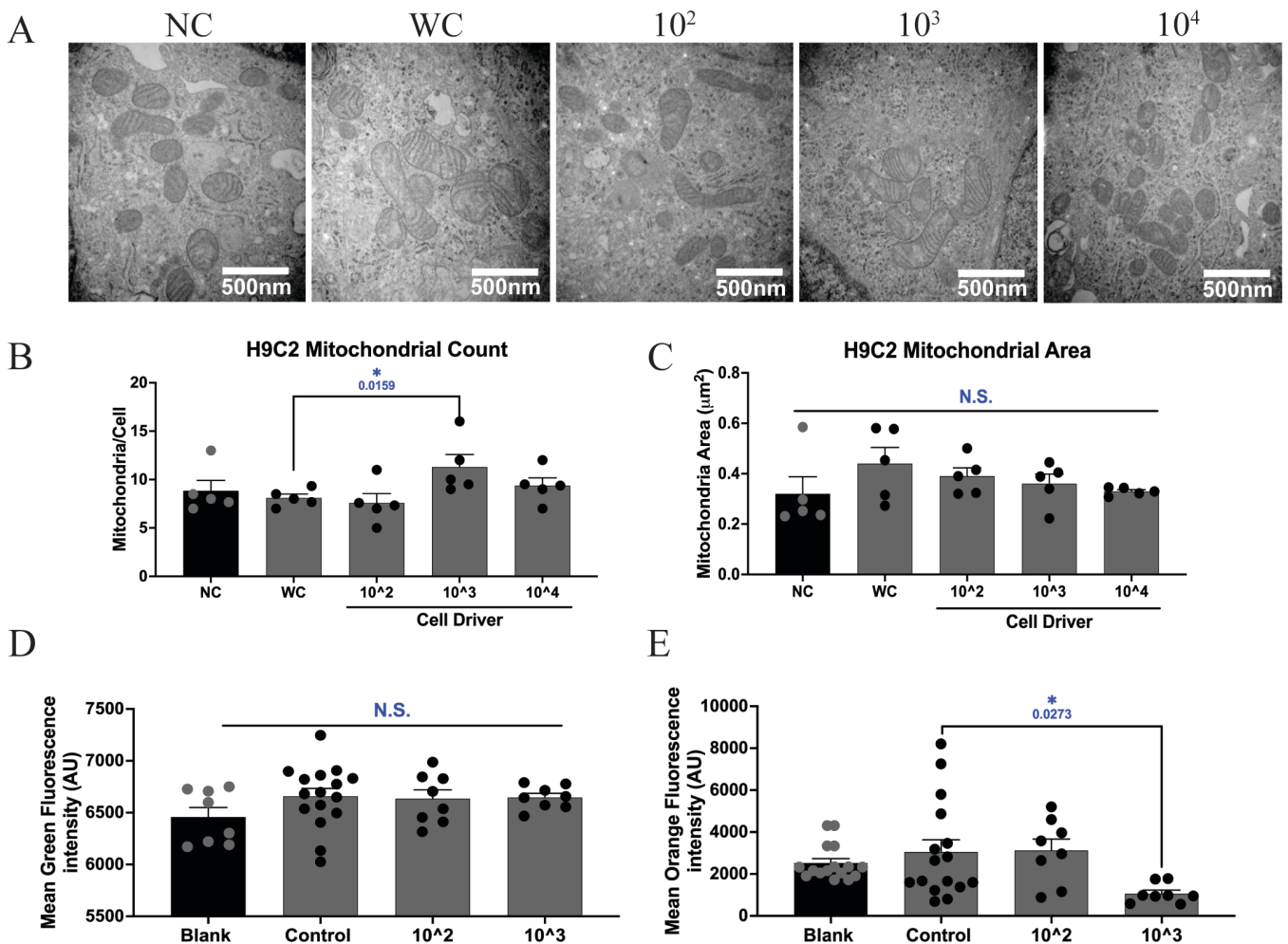


**Figure 2:** CD infoceutical does not disrupt mitochondrial structural parameters. (A) Mitochondrial electron micrography of H9C2 cells after controls and CD dilutions. (B) Mitochondrial count *per* cell (n=5). (C) Mitochondrial area ( $\mu\text{m}^2$ ) (n=5). \*p<0.05, compared with NC. (D) Green and orange (E) signals after ED3 imprinting. \*p<0.05, compared with control.

consequences in the field of regeneration. To investigate the effect of infoceutical waters on proliferation of neural stem cells, neurospheres were cultured for 72 hours with daily addition of control, energy, or COH infoceuticals at various dilutions. Cells were then dissociated and cultured with 5-Bromo-2'-deoxyuridine (BrdU) for 24 hours to assess neural stem cell proliferative capacity. While we saw no significant effect on proliferation using Energy water (data not shown). We observed an increase in cellular proliferation after the chronic treatment (72h) with COH at  $10^3$  dilution (Fig 3). However, we do see a slight increase in

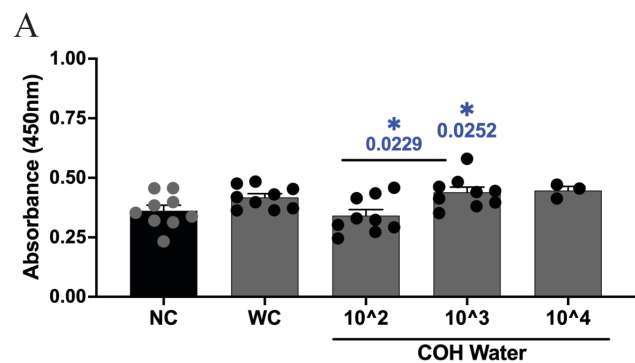


**Figure 3:** COH infoceutical increases cellular proliferation of neuronal stem cells. (A) Cellular proliferation of neural stem cell after COH treatment. \*p<0.05, compared with NC.

proliferation using the control water, which is consistent with data from other experiments. These results indicate that COH has a positive effect on proliferation of neural stem cells suggesting the potential benefit of this infoceutical in the stem cell biology field.

### ***ET3 infoceutical protects lung epithelial cells from respiratory virus infection.***

Considering the structural changes observed, we decided to investigate the possible protective effect of the immune ET3 infoceutical against viral infections. For this purpose, we design an engineered Sars-Cov2 virus and evaluate lung epithelial cells (A549) infection. We observed that when cells were treated for 72h with ET3, a reduction in viral infection was observed (**Fig. 4**). This result suggests that ET3 immune infoceutical treatment may induce cellular adaption that reduces viral infection.

### ***ED3 frequency imprinting improves mitochondrial health and promotes viral infection protection.***

Elevations in levels of ROS have been associated with cellular damage. Thus, we treated cells with ED3 imprinting followed by measures of cellular ROS by fluorescence of CellROX dye, which produces a strong green fluorescence signal in the presence of high levels of ROS. When H9C2 cells were treated with ED3 frequency imprinting, a significant reduction in the ROS signal was observed, compared with the control ( $p=0.0079$ ) (**Fig. 5A**), suggesting that this frequency may induce a cellular oxidative stress reduction. In addition, the same imprinting treatment induces an improvement in mitochondrial health by means of mitochondrial membrane potential (**Fig. 5 B, D**).

To evaluate the potential that ED13 infoceutical imprinting frequency might have in the host-pathogen interaction, we evaluated the potential to protect lung epithelial cells from viral infection. When A-549 cells were treated with

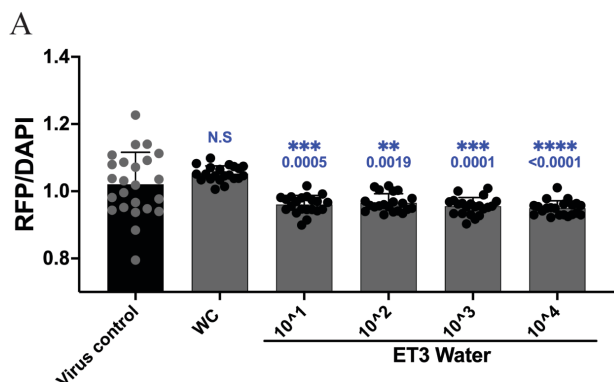


**Figure 4: ET3 immune infoceutical protects from pseudo-Covid virus infection. (A)** Pseudovirus infection after ET3 immune infoceutical treatment. \* $p<0.05$ , compared with NC.

ED13, we observed a significant reduction in the RFP/DAPI ration for the Beta ( $0.90\pm0.024$ ,  $p<0.0001$ ), Delta ( $0.89\pm0.027$ ,  $p<0.0001$ ), D614G ( $0.91\pm0.028$ ,  $p<0.0001$ ), and Lambda ( $0.90\pm0.036$ ,  $p<0.0001$ ) variants (**Fig. 5C**). However, the original strain (Pseudovirus) and UK variant present an increase in viral infection. In addition, when we performed immunofluorescence microscopy, we observed that, in line with previous results, the red signal was reduced in the A549 cells that were treated with ED13 imprinting (**Fig. 5E**). These results suggest that the ED13 imprinting triggered a protective effect that is strain specific.

## Discussion

In this study, the aim was to investigate the effects of various infoceuticals and energetic imprinting on cellular physiology and behavior. We used several different infoceuticals each of which contains unique types of information. These infoceutical waters were prepared by NES Health parameters [6]. Cell Driver (ED3) serves for cellular energy, metabolism, and communication and matches with various immune cells, including mast cells and immunoglobin E. Muscle Driver (MD9) matches muscles, joints, and connective tissue but not

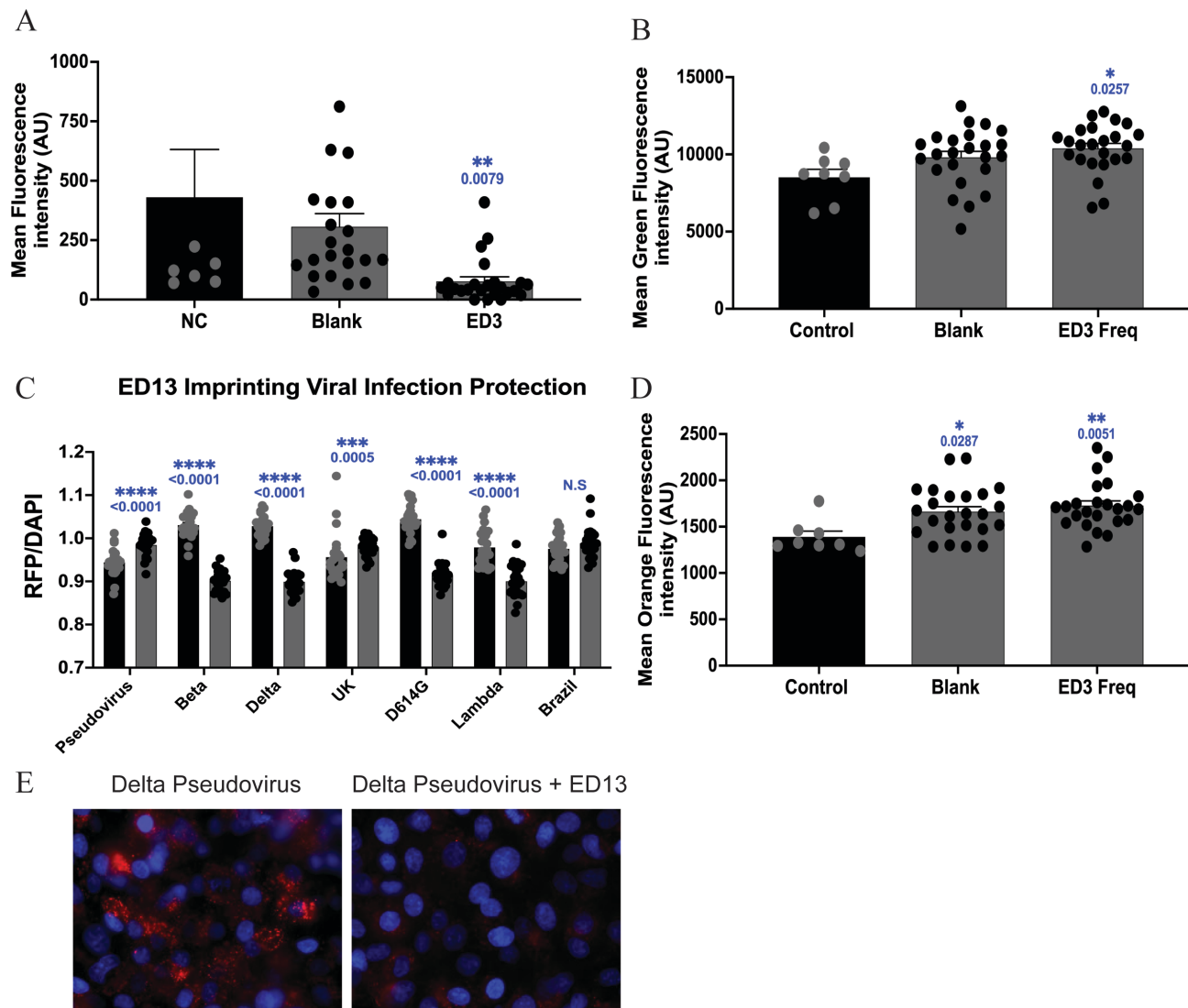


**Figure 5: Frequency imprinting improves mitochondrial health and protects against viral infection.** (A) CellROX green signal in H9C2 cells after ED3 imprinting during 72h. \* $p<0.05$ , compared with control. (B) Green and orange (D) signals after ED3 imprinting. \* $p<0.05$ , compared with control. (C) Cellular infection by the original pseudo virus and the Beta, Delta, UK, D614G, Lambda, and Brazil variants. Black column, virus control; grey column, ED13 imprinting+virus. (E) Immunofluorescence of A549 cells with Delta pseudovirus infection (**left panel**) and with ED13 infoceutical treatment (**right panel**). Red, RFP signal that reports cells that were infected; blue, nuclear staining. Scale bar: 10mm.

heart muscle. It serves for muscle growth, repair and metabolism, maturation of monocytes, and restores muscle trauma and stress. COH (ES13) bioenergetically links to carbon, oxygen, and hydrogen and is central to physiology, especially in their roles in carbohydrate and sugar metabolism, regulating the body's energy use. It

supports toxin excretion, functions of hormones and enzymes, and correlates to Adenosine triphosphate (ATP) production.

Cellular membranes can be considered as an organelle with complex functions and deep implications for cell physiology rather than simply housing organelles. In this regard, we

studied membrane biophysical parameters after treating with Cell Driver in order to determine the impact on membrane structure and, consequently, its function. We used 5-DSA, which is a probe commonly used to assess membrane rigidity and fluidity parameters near the polar head groups. Our data suggest that there is an increase in the rigidity/fluidity ratio when we use a high dilution of Cell Driver. The increase in this ratio is associated with a more organized membrane. In other words, when this ratio is higher, it is expected that freely moving proteins in the membrane are more organized and thus better able to carry out membrane-specific functions.

Additionally, we measured the membrane fluidity in the hydrophobic core of the membrane by using 16-DSA. Interestingly, we observe an increase in the fluidity near the center of the membrane (smaller rotation correlation time; Fig 1D). The center of the hydrophobic core of the membrane is fluid by nature, and it is known that nonpolar molecules can cross through the membrane. Thus, an increase in the fluidity of the hydrophobic core may facilitate the transport of nonpolar molecules such as oxygen [2]. The changes reported here are mostly structural; therefore, further experiments must be done in order to definitively conclude what the functional impact is due to these biophysical shifts.

Mitochondria have long been considered the ‘powerhouse of the cell’ due to the production of ATP, which is the cell’s energy currency. The generation of ATP is dependent on both the physical ultrastructure of the mitochondria as well as its metabolic function. We first tested the Cell Driver infoceutical in H9C2 cells and analyzed mitochondria ultrastructure by electron microscopy. We observed no overall changes in the structure, number, or area of the mitochondria compared with controls (Fig 2A-C). While we do see a slight elevation in the number of mitochondria per cell at a lower dilution of the Cell Driver, these results would suggest the infoceuticals are neither toxic nor beneficial to

the mitochondrial structure. In addition to these measures, quantification of the mitochondrial membrane potential (MMP) is critical for us to understand general mitochondrial health. We measured the MMP by using two signals (described in the methods) where the green fluorescence signal is an indicator of the loss of MMP, whereas the orange signal refers to a healthy mitochondrion. When the MMP of H9C2 cells following treatment with Cell Driver infoceutical was tested, we unexpectedly observe no decrease in MMP (i.e. no increase in green fluorescence) but we also do not observe the corresponding increase in mitochondrial health (i.e. orange fluorescence) (Fig 2D, E). This suggests, again, that the infoceutical is neither toxic nor greatly beneficial to the mitochondria.

Mitochondria also plays a critical role in many other cell types in the body, including neural stem cells (NSCs). NSCs exist in the adult brain in two discrete microenvironments: the subventricular zone and the dentate gyrus (DG) of the hippocampus. The hippocampus is a region of the brain that is critical for learning and memory performance, as well as anxiety and depressive behaviors. It was thought for many years that the adult brain does not produce new neurons. However, evidence has been emerging since the early 2000s that not only do these cells differentiate into functional neurons in the hippocampus, but they are also critical for learning and memory performance in the adult brain [9, 10].

As NSCs go through the process of self-renewal, migration, and differentiation, there are specific morphological and molecular markers that are expressed that allow researchers to trace and classify what types of neural cells these NSCs become. Many of these *in vivo* studies rely on the incorporation of BrdU, a thymidine analog, to investigate the extent of neurogenesis in the adult brain [11]. To investigate proliferative properties *in vitro*, BrdU incorporation is a reliable and commonly utilized assay [12-14]. In this study, NSCs were cultured

in the presence of BrdU for 24 hours following a 72-hour exposure to the infoceuticals. We observe an increase in proliferation in the presence of COH (Fig 3) but not with the other infoceuticals tested. This supports the idea that the infoceuticals differentially affect cell types, as observed here. Given that COH is thought to impact cellular metabolism and that metabolism itself can directly affect cellular proliferation, it is possible that this may be why we see a differential effect in this cell type. Further investigation is necessary to determine why this is the case, as well as to determine the behavior of mitochondria in these cells. Future experiments that determine why infoceuticals differentially affect cells and, additionally, if they have the potential to affect the differentiation of NSCs will be of great interest.

It is also of great interest to investigate the quantifiable effectiveness of a holistic approach to preventing infection. Here we investigated if infoceutical treatment could confer cellular protection against infection of the SARS-CoV-2 virus. In this experiment, we used a pseudovirus that induces RFP expression in cells that have taken up the virus. Excitingly, there is decreased expression of RFP in cells treated with the Immune water (ET3) infoceutical indicating decreased viral infection of the COVID-pseudovirus (Fig 4). These results suggest that treatment with Immune water (ET3) confers protection against SARS-CoV-2 viral infection. Given these observed biological changes following infoceutical treatment, which are beneficial to cellular health and immune response, it is critical for more extensive studies to be performed in order to fully understand the mechanism underlying them.

Lastly, we wanted to understand if the benefit observed using the infoceutical waters could be replicated using an imprinter that could impart information directly onto the cells. First, we measured the generation of ROS, which is associated with cellular oxidative damage. ROS are common signaling molecules; however, when

levels of ROS are outside of the normal range, these species can become toxic to the cell. Our data shows that the ED3 imprinting significantly reduced ROS production, which implies that there is a protective effect (Fig 5A). Second, we quantified the fluorescent signals associated with MMP (i.e. mitochondrial health). While we see a very slight increase in green fluorescence with ED3 imprinting, we see a much more robust response of orange fluorescence, which reflects an increase in MMP (Fig 5B, D). This would suggest that imprinting has the ability to be as effective as infoceutical water treatment. Thirdly, we quantified the ability of the SARS-CoV-2 pseudovirus and its variants to infect lung epithelial cells following imprinter exposure. While we do see some increase in the original pseudovirus, we observe significant decreases in RFP signal of the COVID variants following imprinting (with the exception of the UK and Brazil variant; Fig 5C). These results would suggest that the imprinting is not only conferring some type of protection against viral infection but also that it is doing so through a unique mechanism. Additional experiments are necessary to fully elucidate these observations.

In summary, this work presents evidence that both the infoceuticals and imprinting may exert positive biological effects on cellular physiology. It is important to note that these effects are not equal between either the type of treatment (water versus imprinting) or cell types. Observations from this study are the first of their kind, and thus more comprehensive experiments are necessary to understand the mechanisms underlying these changes.

### Acknowledgement

We acknowledge Ingrid Niesman electron microscopy image generation at the SDSU EM Facility in the Department of Biology.

## Literature Cited

1. Ray, S., et al., *The plasma membrane as a capacitor for energy and metabolism.* Am J Physiol Cell Physiol, 2016. **310**(3): p. C181-92.
2. Zuniga-Hertz, J.P. and H.H. Patel, *The Evolution of Cholesterol-Rich Membrane in Oxygen Adaption: The Respiratory System as a Model.* Front Physiol, 2019. **10**: p. 1340.
3. Van Hal M, D.A., Green MS. Acupuncture. [Updated 2021 Jul 31]. In: StatPearls [Internet]. Treasure Island (FL): StatPearls Publishing; 2022 Jan-. Available from: <https://www.ncbi.nlm.nih.gov/books/NBK532287/>.
4. Wang, T.H., et al., *Comparison of physical electrical conductivity and acupuncture de-qi sensation between stainless steel needling and supercritical fluid-treated needling.* Biomed J, 2021. **44**(6 Suppl 2): p. S267-s274.
5. Fraser, P.H., *Energy and Information in Nature.* 2012: Choice Point Communications. Peter H. Fraser.
6. Massey, H., *Energy for Life: how to charge your body battery and optimize your control system.* 2019: NES Health®.
7. Bonds, J.A., et al., *Deficits in hippocampal neurogenesis in obesity-dependent and -independent type-2 diabetes mellitus mouse models.* Sci Rep, 2020. **10**(1): p. 16368.
8. Ogura, R., et al., *ESR spin-labeling method of determining membrane fluidity in biological materials--tissue culture cells, cardiac mitochondria, erythrocytes and epidermal cells.* Kurume Med J, 1988. **35**(4): p. 171-82.
9. Yao, J., Y. Mu, and F.H. Gage, *Neural stem cells: mechanisms and modeling.* Protein Cell, 2012. **3**(4): p. 251-61.
10. Lazarov, O. and R.A. Marr, *Neurogenesis and Alzheimer's disease: at the crossroads.* Exp Neurol, 2010. **223**(2): p. 267-81.
11. Ivanova, A., et al., *Synthetic Thymidine Analog Labeling without Misconceptions.* Cells, 2022. **11**(12).
12. Demars, M., et al., *Impaired neurogenesis is an early event in the etiology of familial Alzheimer's disease in transgenic mice.* J Neurosci Res, 2010. **88**(10): p. 2103-17.
13. Gao, J., et al., *In vitro investigation of the mechanism underlying the effect of ginsenoside on the proliferation and differentiation of neural stem cells subjected to oxygen-glucose deprivation/reperfusion.* Int J Mol Med, 2018. **41**(1): p. 353-363.
14. Si, Z., et al., *Heme Oxygenase 1 Inhibits Adult Neural Stem Cells Proliferation and Survival via Modulation of Wnt/beta-Catenin Signaling.* J Alzheimers Dis, 2020. **76**(2): p. 623-641.